

# SANDIA REPORT

SAND92-2449 • UC-742

Unlimited Release

Printed December 1992

AD-A275 412



(L)

## Precision Linear Shaped Charge Designs for Severance of Aluminum Materials

**S** DTIC  
ELECTE  
JAN 3 1 1994  
**A**

Manuel G. Vigil

Prepared by  
Sandia National Laboratories  
Albuquerque, New Mexico 87185 and Livermore, California 94550  
for the United States Department of Energy  
under Contract DE-AC04-76DP00789

This document has been approved  
for public release and sale; its  
distribution is unlimited.

94-02933



94 1 31 006

Issued by Sandia National Laboratories, operated for the United States Department of Energy by Sandia Corporation.

**NOTICE:** This report was prepared as an account of work sponsored by an agency of the United States Government. Neither the United States Government nor any agency thereof, nor any of their employees, nor any of their contractors, subcontractors, or their employees, makes any warranty, express or implied, or assumes any legal liability or responsibility for the accuracy, completeness, or usefulness of any information, apparatus, product, or process disclosed, or represents that its use would not infringe privately owned rights. Reference herein to any specific commercial product, process, or service by trade name, trademark, manufacturer, or otherwise, does not necessarily constitute or imply its endorsement, recommendation, or favoring by the United States Government, any agency thereof or any of their contractors or subcontractors. The views and opinions expressed herein do not necessarily state or reflect those of the United States Government, any agency thereof or any of their contractors.

Printed in the United States of America. This report has been reproduced directly from the best available copy.

Available to DOE and DOE contractors from  
Office of Scientific and Technical Information  
PO Box 62  
Oak Ridge, TN 37831  
Prices available from (615) 576-8401, FTS 626-8401

Available to the public from  
National Technical Information Service  
US Department of Commerce  
5285 Port Royal Rd  
Springfield, VA 22161  
NTIS price codes  
Printed copy: A03  
Microfiche copy: A01

## PRECISION LINEAR SHAPED CHARGE DESIGNS FOR SEVERANCE OF ALUMINUM MATERIALS

DTIC QUALITY INSPECTED 8

Manuel G. Vigil  
Explosive Components Department  
Sandia National Laboratories  
Albuquerque, New Mexico 87185

Accession For		
NTIS	CRA&I	<input checked="" type="checkbox"/>
DTIC	TAB	<input type="checkbox"/>
Unannounced		<input type="checkbox"/>
Justification .....		
By .....		
Distribution /		
Availability Codes		
Dist	Avail and/or Special	
A-1		

### Abstract

The Precision Linear Shaped Charge (PLSC) design concept involves the independent fabrication and assembly of the liner (wedge of PLSC), the tamper/confinement, and explosive. The liner is the most important part of an LSC and should be fabricated by a more quality controlled, precise process than the tamper material. Also, this concept allows the liner material to be different from the tamper material. The explosive can be loaded between the liner and tamper as the last step in the assembly process rather than the first step as in conventional LSC designs. PLSC designs are shown to produce increased jet penetrations in given targets, more reproducible jet penetration, and more efficient explosive cross sections using a minimum amount of explosive. The Linear Explosive Shaped Charge Analysis (LESCA) code developed at Sandia National Laboratories has been used to assist in the design of PLSCs. LESCA predictions for PLSC jet penetration in aluminum targets, jet tip velocities and jet-target impact angles are compared to measured data.

## Contents

Introduction .....	7
General Linear Shaped Charge .....	7
Conventional Linear Shaped Charge .....	8
Precision Linear Shaped Charge .....	8
Linear Explosive Shaped Charge Analysis (LESCA) Code .....	9
"Flange" Type PLSC Results .....	10
"W" Type PLSC Results .....	11
Conclusions .....	12
References .....	13-14

## Tables

I LSCAP Versus Experimental PLSC Parameters .....	15
II PLSC Jet Penetration of Aluminum Target Data .....	16

## Figures

1 LSC Cross-Section Variables .....	17
2 Linear Shaped Charge Collapse and Jetting .....	18
3 Conventional LSC Fabrication .....	19
4 Conventional 25 gr/ft, Al Sheath, HNS Explosive .....	20
5 Test-to-Test Reproducibility of Conventional LSC .....	21
6 PLSC Components .....	22
7 LESCA Code Model of LSC Cross Section .....	23
8 LESCA Jet Penetration Graphics .....	24
9 Photographs of LSC Jet Tip Envelope Angle and Jet Particle Velocity Vector .....	25
10 LESCA Code Graphical Representation of Half of the LSC Liner Collapse Process .....	26
11 LESCA Code LSC Simulation with Detonator at Minimum versus Maximum Standoff .....	27
12 "Flange" Type 25 gr/ft PLSC .....	28
13 Conventional LSC Predicted Jet Penetration versus Standoff Compared to Experimental Data .....	29
14 Jet Penetration in Aluminum versus Standoff for PLSC versus Conventional LSC (Al Liner, 90 degree apex, Al Tamper) .....	30
15 65 gr/ft, PLSC7 Actual Cross Section .....	31

## Contents (continued)

16	65 gr/ft, PLSC7 Cross Section and Jet Penetration into Aluminum 6061-T6 versus Standoff (LESCA versus Measured Data) .....	32
17	20 gr/ft PLSC Jet Penetration in 6061-T6 Aluminum versus Standoff (LESCA versus Measured Data) .....	33
18	30 gr/ft PLSC6 Jet Penetration versus Standoff (LESCA Code versus Measured Data).....	34
19	Reproducibility of Measured 30 gr/ft PLSC Jet Penetration versus Standoff Data (Two Tests).....	35
20	Reproducibility of 30 gr/ft PLSC6 Jet Penetration versus Distance Along Target (Constant Standoff, Foam Tamper) .....	36
21	PLSC Jet Penetration Depth (P) versus PLSC Explosive Loading (G) for Aluminum Targets .....	37

## **Precision Linear Shaped Charge Designs for Severance of Aluminum Materials**

### **Introduction**

Sandia National Laboratories (SNL)<sup>1-9</sup> is involved in the design of Linear Shaped Charge (LSC) components varying in size from 10 to 10,500 gr/ft. These LSC components are required to perform such functions as rocket stage separation, parachute deployment, parachute system release, flight termination, system destruct, bridge destruction, and system disablement. Most of the LSC components for these systems require precise and reproducible jet penetration using the minimum explosive and component weights.

Sandia National Laboratories is currently involved in a task to design Precision Linear Shaped Charges (PLSC).<sup>1-9</sup> The sweeping detonation and 3-dimensional collapse process of an LSC is a complex phenomenon. The Linear Shaped Explosive Charge Analysis (LESCA) code was developed at SNL to assist in the design of PLSC components. Analytical output from the LESCA code is presented and compared to experimental data for various PLSC designs in the 16 to 10,500 gr/ft explosive loading range. The LESCA code models the motion of the LSC liner elements due to explosive loading, jet and slug formation, jet breakup, and target penetration through application of a series of analytical approximations. The structure of the code is intended to allow flexibility in LSC design, target configurations, and in modeling techniques. The analytical and experimental data presented include LSC jet penetration in aluminum targets as a function of standoff, jet tip velocities and jet-target impact angles.

### **General Linear Shaped Charge**

The parameters or variables for a general linear shaped charge cross section are illustrated in Figure 1. The large number of variables defining a cross section makes the design of "the" optimum LSC a very difficult task. Therefore, the scaling of LSCs is not a simple task. The larger core explosive loading (gr/ft) of similar LSCs from the same manufacturer do not necessarily produce deeper jet penetrations in a given target. The generic operational characteristics of an LSC are shown in Figure 2. A metal tube or sheath containing explosive is formed so that a wedge is created on one side. The LSC is typically point- or end-initiated and a detonation wave propagates along the axis. The wedge collapses on itself and forms a high velocity sheet of jet particles. In general the jet particles are not projected perpendicular to the original direction of the liner nor is the particle velocity perpendicular to the jet front.

The leading, relatively high velocity (3-5 mm/ $\mu$ s), main jet produces most of the jet penetration into the target. The slower (1-1.5 mm/ $\mu$ s) rear jet or slug is usually found embedded in the cavity generated in the target by the main jet. Severance of a finite thickness target results from both the penetration of the main jet and the fracture of the remaining target thickness. The fracture portion of the severed thickness usually varies and can be up to 50% depending on the target strength parameters.

### **Conventional Linear Shaped Charge**

Typically, conventional LSCs are fabricated by loading a cylindrical tube with granular explosives, and then roll- or swage-forming the loaded tube to the familiar chevron configuration illustrated in Figure 3.

Some of the disadvantages of conventional LSC designs are as follows:

1. Nonsymmetrical cross section,
2. Nonuniform explosive density,
3. Nonoptimized explosive and sheath cross sections, and
4. Historically designed for nonprecise jet cutting.

The explosive and sheath cross section of a conventional 25 gr/ft, aluminum sheathed LSC loaded with HNS II explosive is shown in Figure 4. Figure 5 illustrates the test-to-test variations in jet penetration of an aluminum target for the 25 gr/ft LSC shown in Figure 4.

### **Precision Linear Shaped Charge**

For PLSC the liner, explosive, and tamper materials can be assembled as illustrated in Figure 6. The liner, tamper, and explosive are manufactured independently to allow the required control of fabrication methods which result in a more precise component. The quality control of the liner is most important in the performance of LSC devices.

An extruded, machined, buttered, or cast explosive is loaded or assembled between the liner and tamper components after these other two components are fabricated. The explosive can be loaded using single or multiple extrusions or by a "buttering" manual technique, if necessary. Assembly aids, such as the use of vacuum, are also useful.

The LESCA code has been used to improve the PLSC parameters. The explosive charge to liner mass ratio can be designed to optimize the transfer of energy from the detonation wave through the liner to the high-velocity jet. The explosive charge to tamper mass ratio can be designed to optimize the tamper material and thickness. The maximum tamper thickness is defined as that thickness beyond which no additional gain in the liner collapse velocity is obtained. The tamper can be made of a different material than that for the liner in order to:

1. Fit different configurations,
2. Allow for buttering of explosive,
3. Allow selection of tamping characteristics in material,
4. Allow for built-in shock mitigation properties, and
5. Allow for a built-in standoff housing free of foreign materials and water which degrade jet formation.

### **Linear Explosive Shaped Charge Analysis (LESCA) Code**

The Linear Shaped Charge Analysis Program (LSCAP) was renamed the Linear Explosive Shaped Charge Analysis (LESCA) code. Therefore, throughout this report, LSCAP and LESCA code modeling, simulation, and predictions are interchangeable.

The modeling capabilities of the LESCA code include:

1. Sweeping/tangential detonation propagation,
2. Jet-target impact angles,
3. Liner acceleration and velocity,
4. Jet formation process,
5. Jet penetration process including layered targets,
6. Jet breakup stress model, and
7. Target strength modeling.

The code is inexpensive relative to hydrocodes, can be easily used to conduct parametric studies, and is interactive. The LESCA modeling of half of an LSC cross section (symmetry is assumed) is illustrated in Figure 7. Figure 8 shows sample LESCA output illustrating an LSC with a variable standoff to an aluminum target, sweeping detonation, a jet front envelope of 26.7 degrees, jet particle path relative to the target, and a comparison of the predicted and experimental target-jet penetration at 8 and 24 microseconds, respectively.



The jet tip envelope angle, theta, and jet particle velocity vector angle, alpha, are shown in Figure 9 for two different LSCs. Measured data from Cordin rotating mirror camera film records were used in the angle comparisons with LSCAP (LESCA) code predictions listed in Table I.

Assuming a symmetrical liner collapse process, typical LESCA code graphical representations are shown in Figure 10 for two different times. The LSC jet, slug, liner, tamper, and detonation product gases are shown in Figure 10.

LESCA code predicted jet penetration versus standoff data are shown in Figure 11 for configurations with the detonator at the minimum versus maximum standoff as illustrated in the top half of Figure 11. Experimental data are also compared to the LESCA code predictions in Figure 11.

### **"Flange" Type PLSC Results**

The "flange" type PLSC design shown in Figure 12 was designed to allow the extrusion of the LX-13 explosive from one end of the liner and tamper assembly. The length that can be extruded varies with the area or size of cavity between the liner and the tamper materials.

#### **25 gr/ft PLSCO**

The LESCA code jet penetration versus standoff data are compared to measured data in Figure 13 for the conventional, 25 gr/ft, LX-13 explosive, copper liner, aluminum tamper LSC cross section shown in the figure. A similar PLSC was designed to compare jet penetration performance with the conventional LSC shown in Figure 13. Aluminum liner and tamper materials were used. The liner apex angle was 90 degrees. The explosive was LX-13 for the PLSC and HNS II for the conventional LSC. The LX-13 and HNS II explosive metal driving ability is about the same. The measured jet penetration into an aluminum 6061-T6 target versus standoff data are compared in Figure 14. The PLSC jet penetration was 40% greater than for the conventional LSC.

A parametric study was conducted incorporating the following variables into the 25 gr/ft, LX-13 explosive, flange PLSC designs similar to Figure 12:

1. Explosives
  - a. LX-13/XTX-8003/PBXN-301
2. Liner materials
  - a. Copper
  - b. Aluminum
  - c. Nickel

3. Tamper/confinement material
  - a. Aluminum
4. PLSC Geometry
  - a. Liner apex angles ( $\beta$ ):  
70, 90 and 105 degrees
  - b. Liner thicknesses (t):  
.004, and .010 inches

The PLSC materials, liner thickness (t), and apex angles ( $\beta$ ) were varied as listed in Table I. The PLSC jet tip velocity ( $V_j$ ), jet envelope angle ( $\Theta$ ), jet-target impact angle ( $\alpha$ ), jet penetration into an aluminum 6061-T6 target (P), and optimum standoff (S.O.) are listed in Table I. The LESCA predicted data are compared to the experimental values for most of the parameters. The effect on jet penetration versus standoff due to variations in some of the PLSC cross-section parameters were published in Reference 1.

#### 65 gr/ft PLSC7

The 65 gr/ft "flange" type PLSC7 cross section is shown in Figure 15. The jet penetration into a thick aluminum (6061-T6) target versus standoff data predicted by the LESCA code are compared to experimental data in Figure 16. The PLSC7 configuration includes a 0.012 inch thick copper liner, LX-13 explosive, and an aluminum tamper.

### **"W" Type PLSC Results**

#### 20 gr/ft PLSC5

The "W" type PLSC design shown in Figure 17 was designed to allow the explosive to be manually loaded in the liner in a buttering technique. This loading technique is required for relatively small PLSC cross sections where long segments are desired. The 20 gr/ft PLSC5, LESCA code predicted, jet penetration versus standoff data are compared to measured data in Figure 17. The PLSC5 configuration includes a 0.008 inch thick copper liner, LX-13 explosive, and aluminum tamper. The apex angle was 75 degrees.

#### 30 gr/ft PLSC6

The "W" type design, 30 gr/ft PLSC6 cross section and copper liner actual cross section are shown in Figure 18. The LESCA-code-predicted jet penetration into an aluminum 6061-T6 target versus standoff data are compared to measured data in Figure 18. The PLSC6 configuration includes a 0.008 inch thick copper liner, LX-13 explosive, an aluminum tamper, and a 77 degree liner apex angle.

The test-to-test reproducibility for the PLSC6 design is illustrated in Figure 19. The measured jet penetration versus standoff data are compared for two tests. The measured jet penetration versus distance along the target data are shown in Figure 20 for two different tests and for a constant standoff of 0.100 inches.

### Conclusions

Precision Linear Shaped Charge liner, tamper, and explosive fabrication processes have been demonstrated to produce increased jet penetrations in aluminum targets, more reproducible jet penetrations, and more efficient explosive cross sections compared to equivalent commercial LSCs.

The LESCA predicted jet tip velocities are within 20% of the experimental values (Table I). The predicted jet envelope angles relative to the PLSC are within 20% of the photometrically measured values (Table I). The measured jet-target angles are within 11% of the predicted values (Table I). Data for PLSC jet penetration into an aluminum target was presented demonstrating a 10% reproducibility for a given test (Figure 20). Data were presented to illustrate 40% improvement in jet penetration for a PLSC design compared to an equivalent 25 gr/ft conventional LSC design (Figure 14).

Jet penetration versus explosive loading data are summarized in Figure 21 and Table II for the PLSC designs for which data were presented in this report. The target material was aluminum 6061-T6. The explosive was LX-13. The tamping material was aluminum, copper or Lexan. The data include both "flange" and "W" PLSC designs. Both "W" and "flange" PLSC designs performed equally well. Data for fracture, which is part of the total severance thickness, of the target was not included in the jet; only penetration data were presented throughout this report.

A parametric study with the LESCA code to determine "the" optimum PLSC design is very difficult because of the large number of interrelated variables. This does, however, emphasize the importance of LESCA in obtaining a more optimized design than is currently available from conventional LSC designs. For a given, new component, once the customer requirements are defined (constraining or fixing some PLSC parameters), then the LESCA code can be used to optimize the remaining parameters.

The PLSC designs similar to those presented here have recently been incorporated in Sandia National Laboratory (SNL) systems. The Explosive Components Department plans to use PLSC designs in all future SNL systems requiring jet severance of materials including metals, Kevlar parachute suspension lines, and graphite-epoxy motor cases.

## References

1. M. G. Vigil, *Design and Development of Precision Linear Shaped Charges*, SAND89-0196C. Proceedings of the 9th International Symposium on Detonation, Portland, OR, August 28-September 1, 1989.
2. M. G. Vigil, J. G. Harlan, *Optimal Design and Fabrication of Reproducible Linear Shaped Charges*, SAND86-0982. Sandia National Laboratories, Albuquerque, NM, 1986.
3. A. C. Robinson, *LESCA - A Code For Linear Shaped Charge Analysis - Users Manual*, SAND90-0150. Sandia National Laboratories, Albuquerque, NM, May 1990.
4. M. G. Vigil, *Design of Linear Shaped Charges Using the LESCA Code*, SAND90-0243. Sandia National Laboratories, Albuquerque, NM, April 1990.
5. M. G. Vigil, *Precision Linear Shaped Charge Jet Severance of Graphite-Epoxy Materials*, SAND92-0610C. Proceedings of NASA Aerospace Pyrotechnic Conference, Houston, TX, June 9-10, 1992.
6. A. C. Robinson, M. G. Vigil, *An Analytical-Experimental Comparison of 150 and 220 Grain Per Foot Linear Shaped Charge Performance*. Tenth International Symposium on Ballistics, San Diego, CA, October 27-29, 1987.
7. A. C. Robinson, *Shaped Charge Analysis Program - User's Manual for SCAP 1.0*, SAND85-0708. Sandia National Laboratories, Albuquerque, NM, April 1985.
8. A. C. Robinson, *Asymptotic Formulas for the Motion of Shaped Charge Liners*, SAND 84-1712. Sandia National Laboratories, Albuquerque, NM, September 1984.
9. A. C. Robinson, *Multilayered Liners for Shaped Charge Jets*, SAND85-2300. Sandia National Laboratories, Albuquerque, NM, December 1985.

Table 1 LSCAP\* Versus Experimental PLSC Parameters  
 Liner: Flange design, phase 0  
 Tamper: Aluminum  
 Explosive: PBXN301, 25 gr/ft, Ensign Bickford  
 Target: Aluminum 6061-T6  
 Cordin Camera: 0.233 us interframe time

Liner Mat.	r(in)	$\theta$ (deg)	$V_j$ (cm/us)		$\theta$ (deg)		$\alpha$ (deg)		P(in)		S.O.(in)		$t_{bm}$ ( $\mu$ s)
			EXP.	LSCAP	EXP.	LSCAP	EXP.	LSCAP	EXP.	LSCAP	EXP.	LSCAP	
AL	.004	70	.57	.65	49	55	62	62	.18	.36	.14	.37	2.6
AL	.004	90	.41	.32	36	26	73	77	.11	.27	.09	.28	NM
AL	.004	105	.38	.46	31	26	84	77	.14	.22	.15	.27	NM
AL	.010	90	.32	.37	28	30	74	75	.14	.15	.17	.17	NM
AL	.010	105	.28	.32	24	26	74	77	.13	.11	.20	.16	3.1
CU	.004	70	.40	.41	22	24	67	78	.11	.41	.15	.16	3.3
CU	.004	90	.36	.33	27	21	77	79	.16	.28	.11	.12	3.1
CU	.004	105	.26	.28	24	19	78	80	.16	.21	.23	.09	NM
CU	.010	70	.23	.25	19	18	80	81	.15	.20	.18	.02	3.1
CU	.010	90	.25	.20	15	16	80	82	.13	.08	.19	.09	NM
CU	.010	105	.15	.17	13	13	85	84	.14	TBD	.23	TBD	NM
NI	.004	90	.33	.33	23	21	74	79	.18	.28	.10	.10	NM
NI	.010	90	.22	.20	15	15	81	83	.11	.09	.15	.08	NM

$V_j$  = jet tip velocity

$\theta$  = jet envelope angle relative to PLSC

$\beta$  = liner apex angle

$t$  = liner thickness

P = jet penetration, maximum

$\alpha$  = jet target impact angle

S.O. = standoff, optimum

Exp. = experimental data

JBREAK = LSCAP jet breakup stress model

TBCON = jet breakup constant

YLIN = dynamic yield stress/liner

Umin = minimum jet penetration velocity

AL = aluminum 6061T6

CU = oxygen free copper/annealed/soft

NJ = annealed/soft/nickel

NM = not measurable

$t_{bm}$  = measured jet breakup time

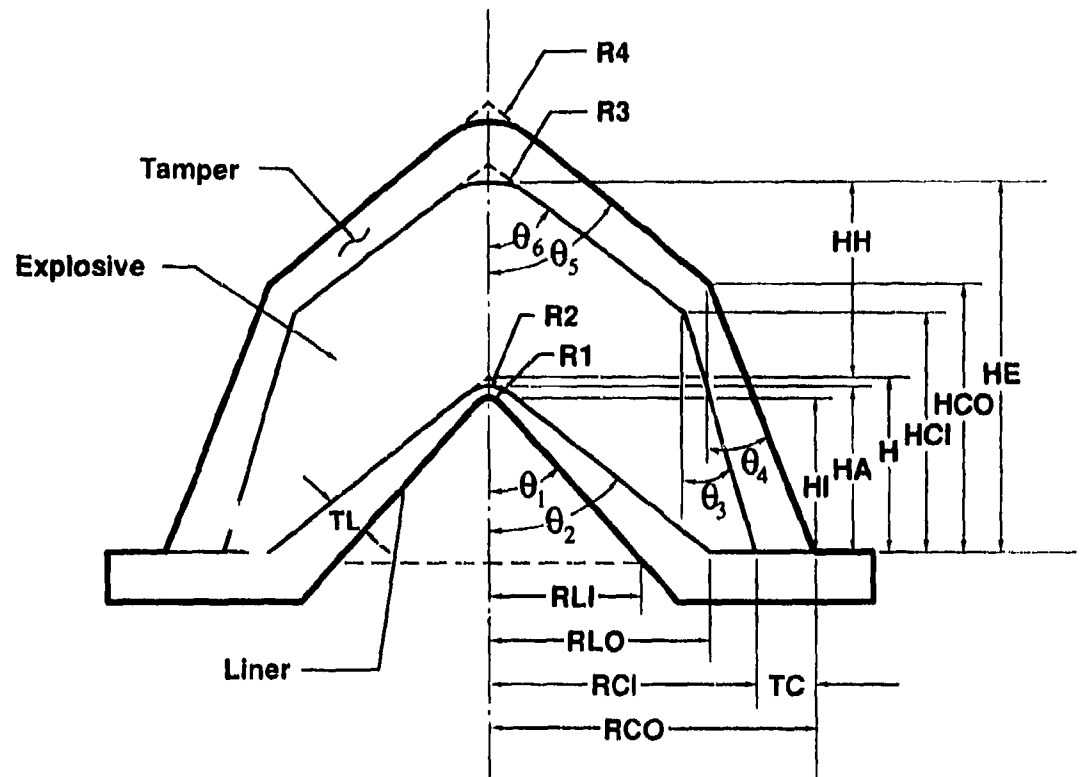
$\alpha = 90 - \theta/2$

\* - LSCAP CODE RENAMED LESCA

**Table II. PLSC Jet Penetration of Aluminum Target Data**

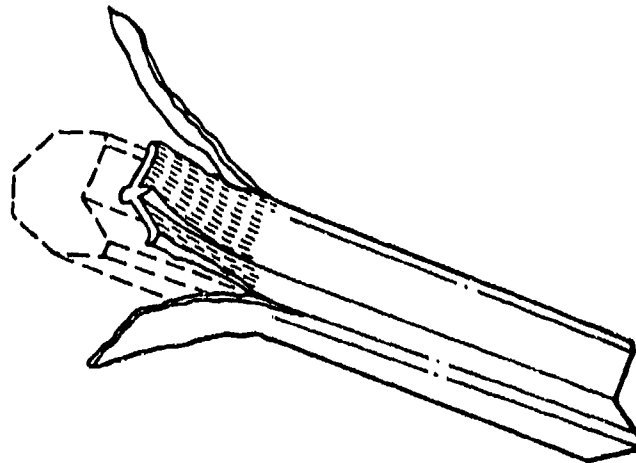
<b>PLSC</b>	<b>(gr/ft)</b>	<b>EXPLOSIVE</b>	<b>TAMPER</b>	<b>TARGET</b>	<b>P (in)</b>	<b>S.O. (in)</b>
0	25	LX-13	Aluminum	6061-T6	0.170	0.100
3	16	LX-13	Aluminum	7075-T6	0.070	0.080
5	20	LX-13	Aluminum	6061-T6	0.130	0.090
6	30	LX-13	Cu/Lexan	6061-T6	0.190	0.100
7	65	LX-13	Aluminum	6061-T6	0.320	0.137

**P - JET PENETRATION DEPTH**  
**S.O. - PLSC STANDOFF FROM TARGET**  
**(gr/ft) - grain/foot EXPLOSIVE LOADING**

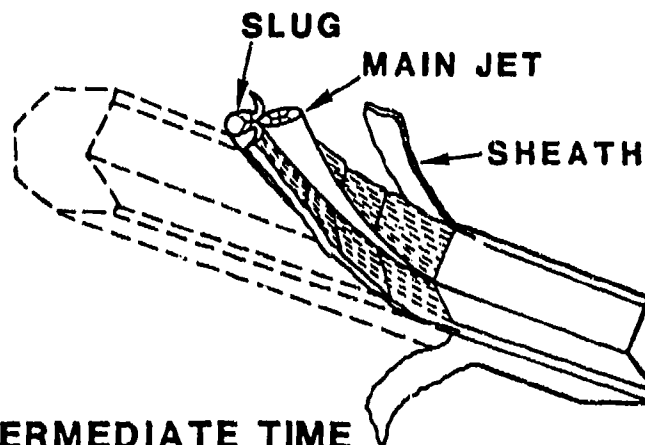


- RLI = LINER INNER RADIUS  
 RLO = LINER OUTER RADIUS  
 RCI = CONFINEMENT/SHEATH INNER RADIUS  
 RCO = CONFINEMENT/SHEATH OUTER RADIUS  
 HI = LINER INNER HEIGHT  
 HA = LINER ACTUAL HEIGHT  
 H = LINER THEORETICAL APEX HEIGHT  
 HCI = CONFINEMENT/SHEATH INNER HEIGHT  
 HCO = CONFINEMENT/SHEATH OUTER HEIGHT  
 HE = EXPOSIVE HEIGHT  
 HH = EXPLOSIVE HEIGHT ABOVE APEX  
 TL = LINER THICKNESS  
 TC = CONFINEMENT/SHEATH THICKNESS  
 R1 = LINER INNER APEX RADIUS  
 R2 = LINER OUTER APEX RADUS  
 R3 = CONFINEMENT/SHEATH INNER APEX RADIUS  
 R4 = CONFINEMENT/SHEATH OUTER APEX RADIUS  
 $\theta_1$  = LINER INNER APEX HALF ANGLE  
 $\theta_2$  = LINER OUTER APEX HALF ANGLE  
 $\theta_3$  = CONFINEMENT/SHEATH INNER APEX HALF ANGLE  
 $\theta_4$  = CONFINEMENT/SHEATH OUTER APEX HALF ANGLE

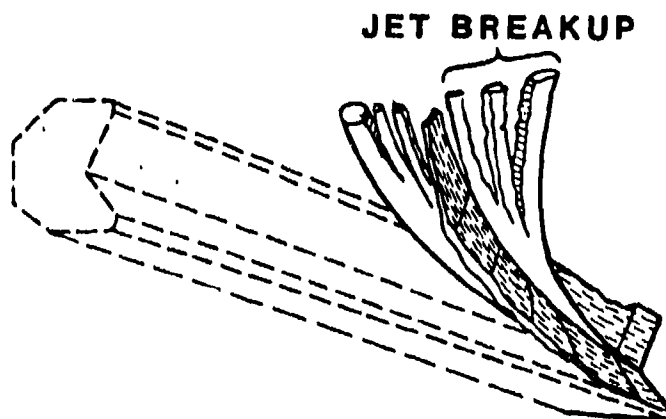
**FIGURE 1. LSC CROSS-SECTION VARIABLES**



(a) INITIAL TIME



(b) INTERMEDIATE TIME



(c) LATE TIME

**FIGURE 2. LINEAR SHAPED CHARGE  
COLLAPSE & JETTING**



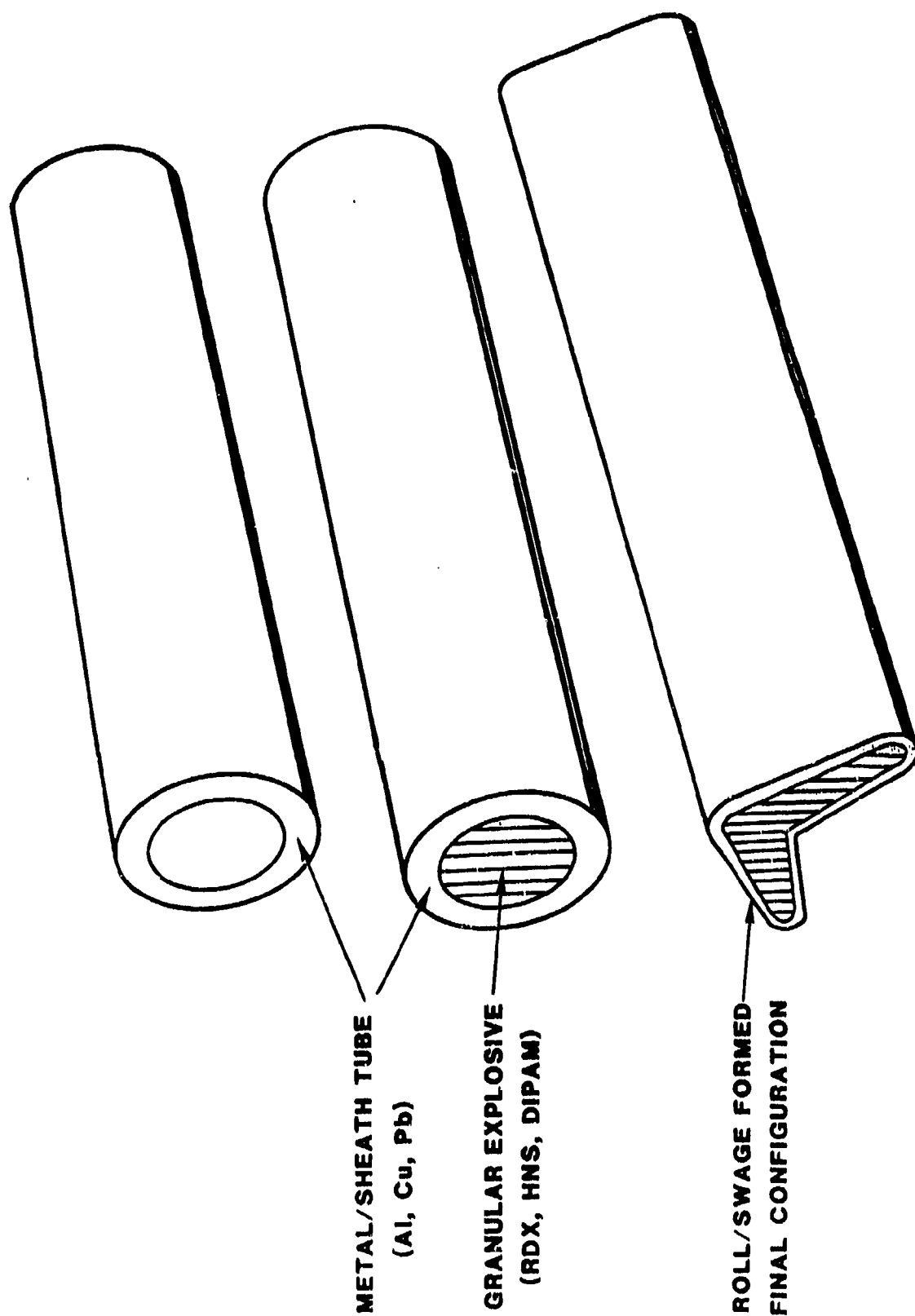


**FIGURE 3. CONVENTIONAL LSC FABRICATION**

MAGNIFICATION - 20X

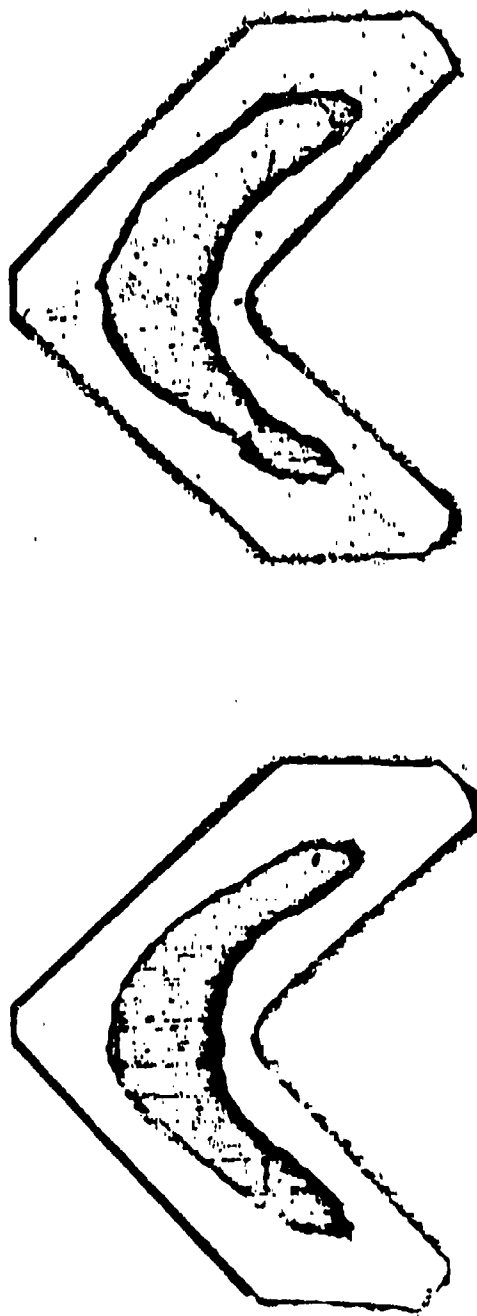


**FIGURE 4. CONVENTIONAL 25 gr/ft, AI SHEATH, HNS EXPLOSIVE  
ACTUAL CROSS-SECTION**

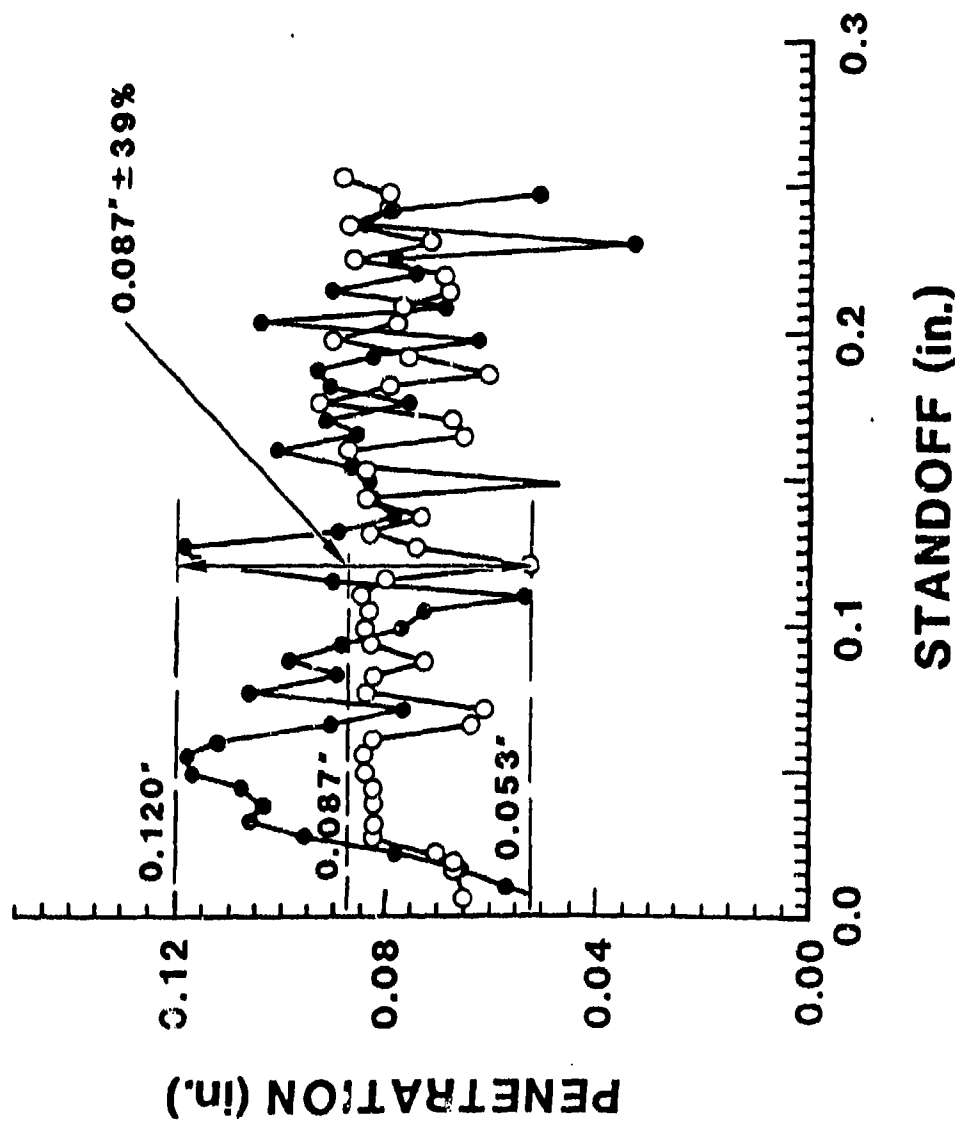


FIGURE 5. TEST TO TEST REPRODUCIBILITY OF CONVENTIONAL LSC

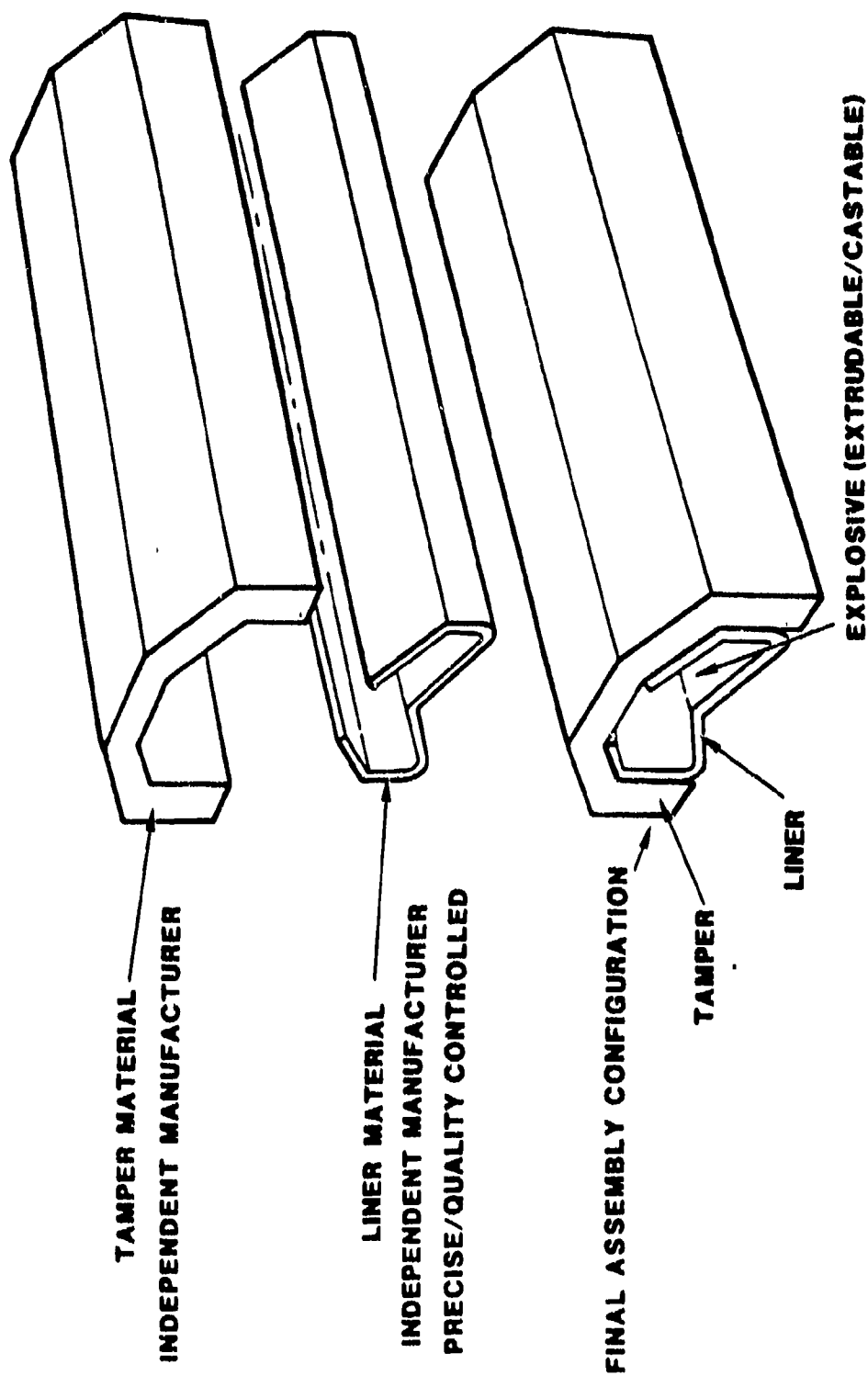


FIGURE 6. PLSC COMPONENTS

25 gr/ft, LX-13 H.E., AL TAMPER, .010" THICK AL LINER

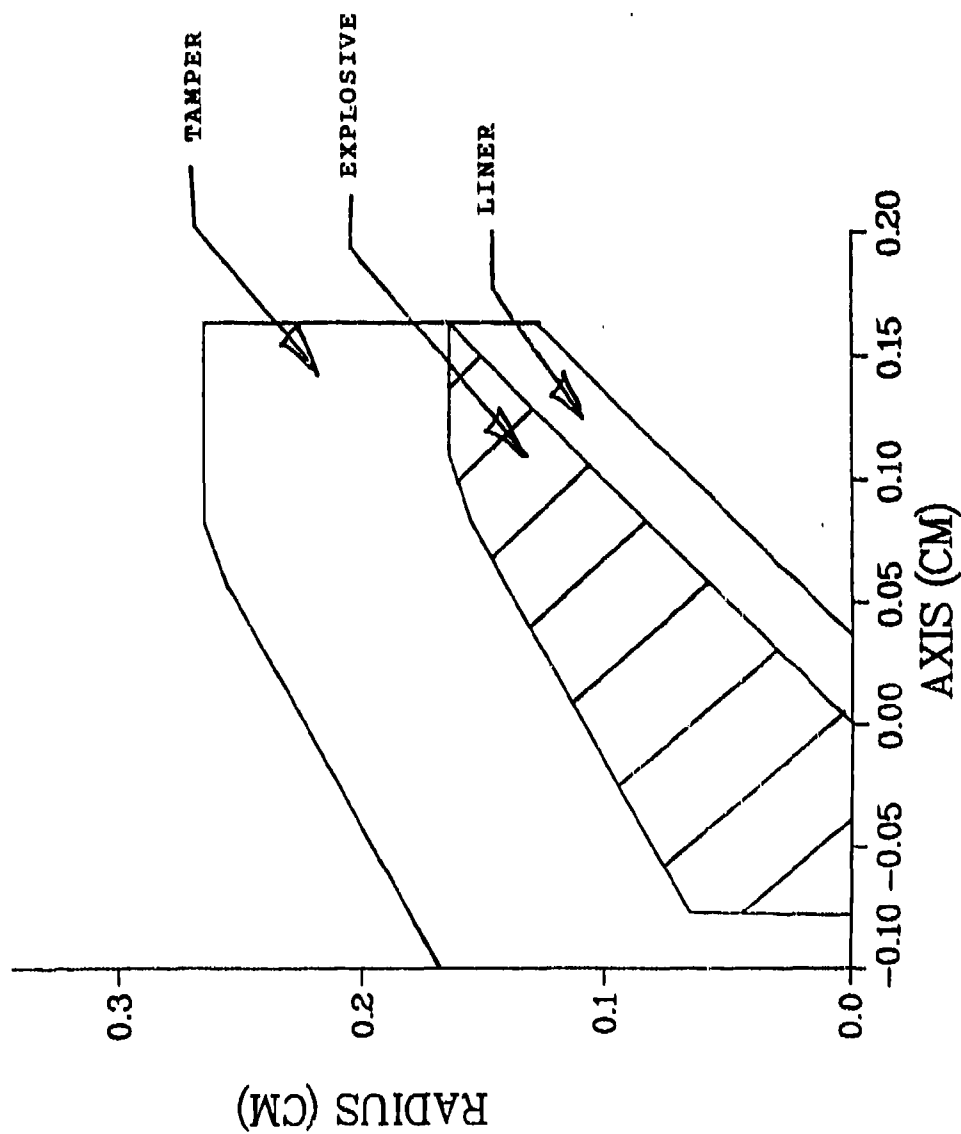


FIGURE 7. LESCA CODE MODEL OF LSC CROSS-SECTION

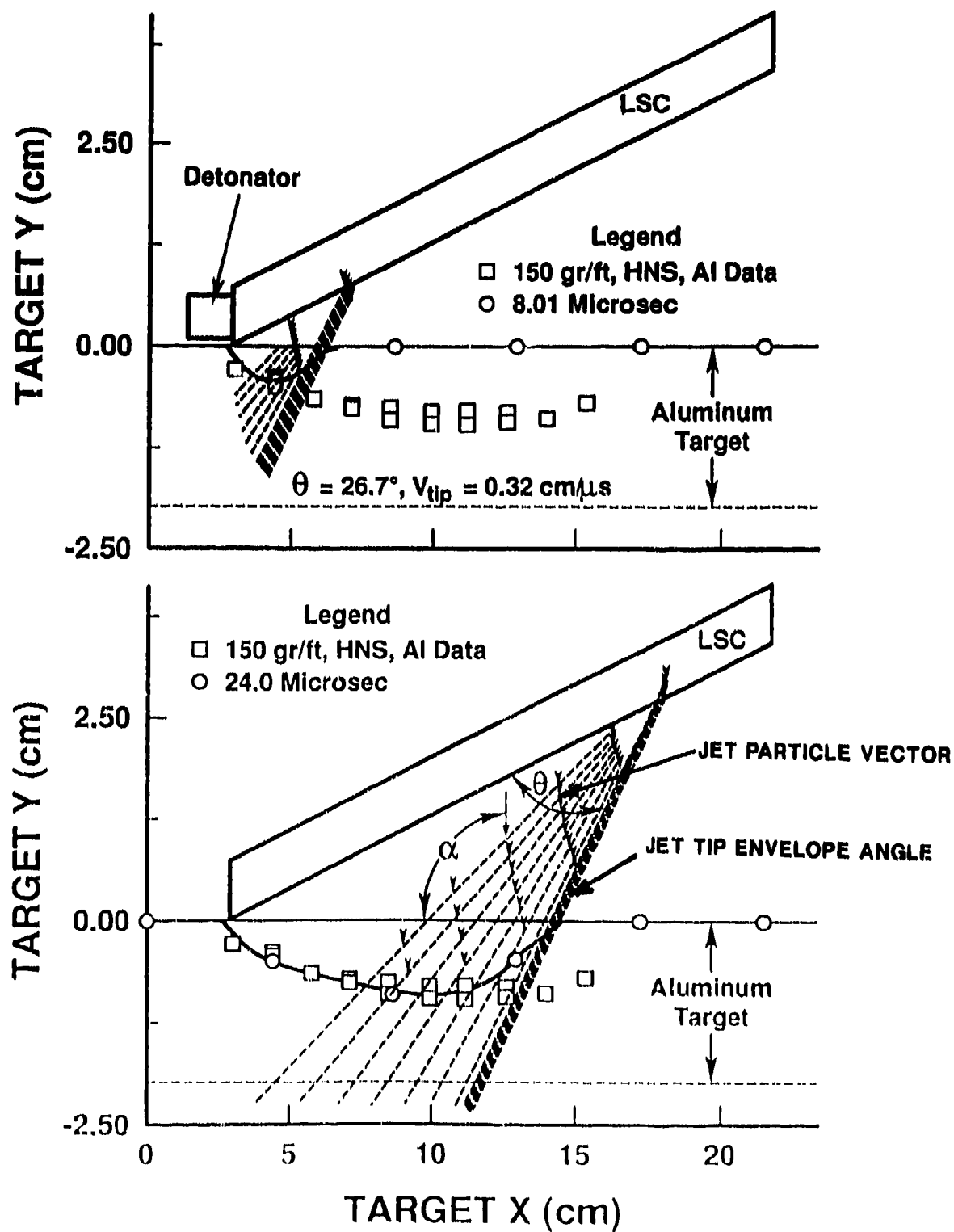


FIGURE 8. LESCA JET PENETRATION GRAPHICS

TA031701.D01

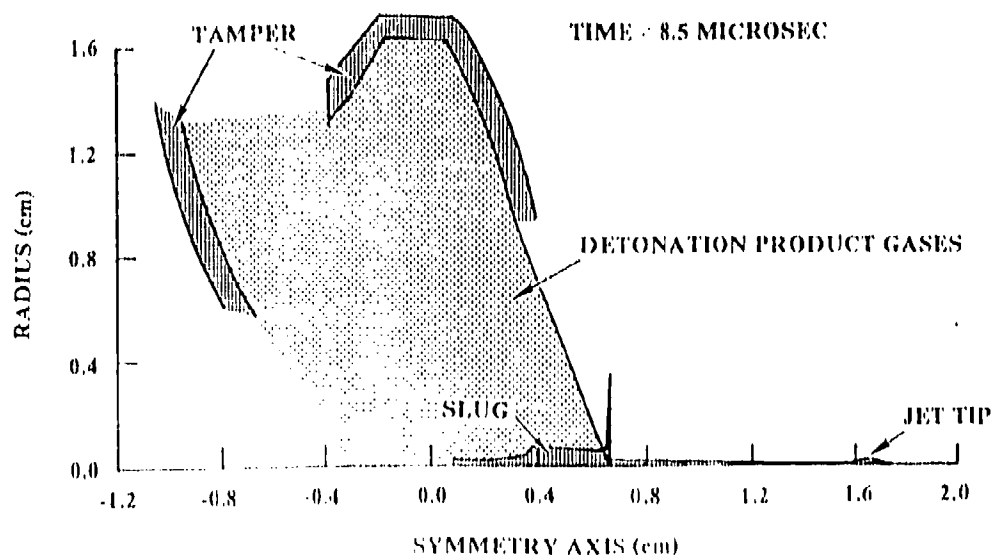
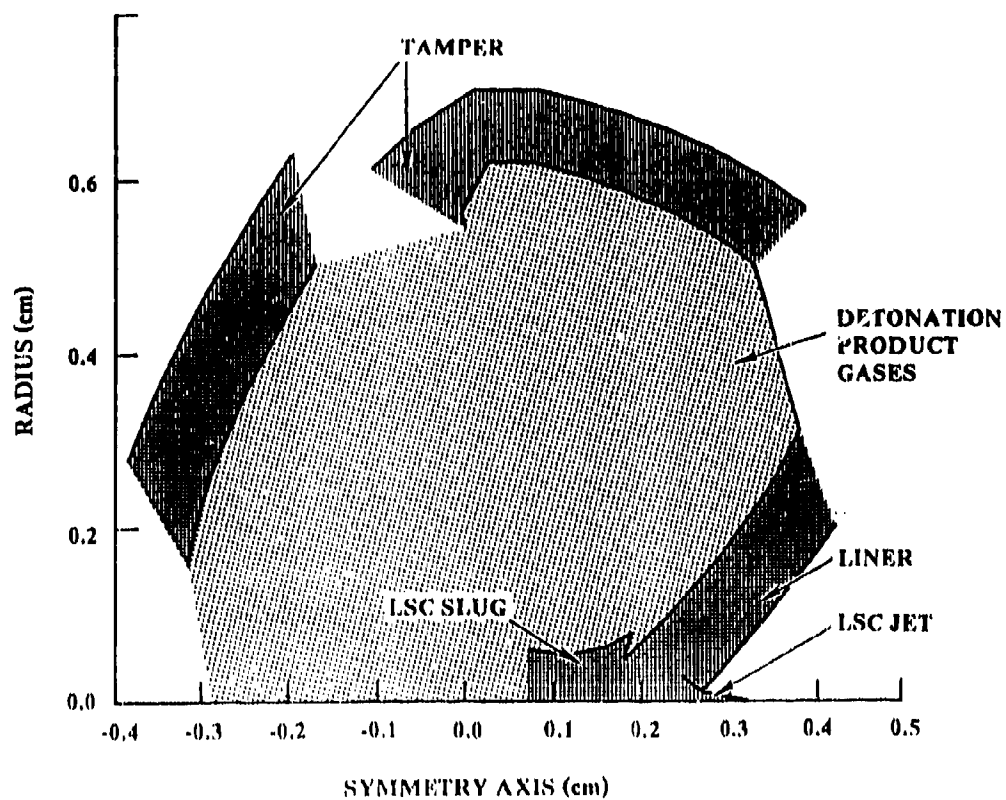


FIGURE 10. LESCA CODE GRAPHICAL REPRESENTATION OF  
HALF OF THE LSC LINER COLLAPSE PROCESS

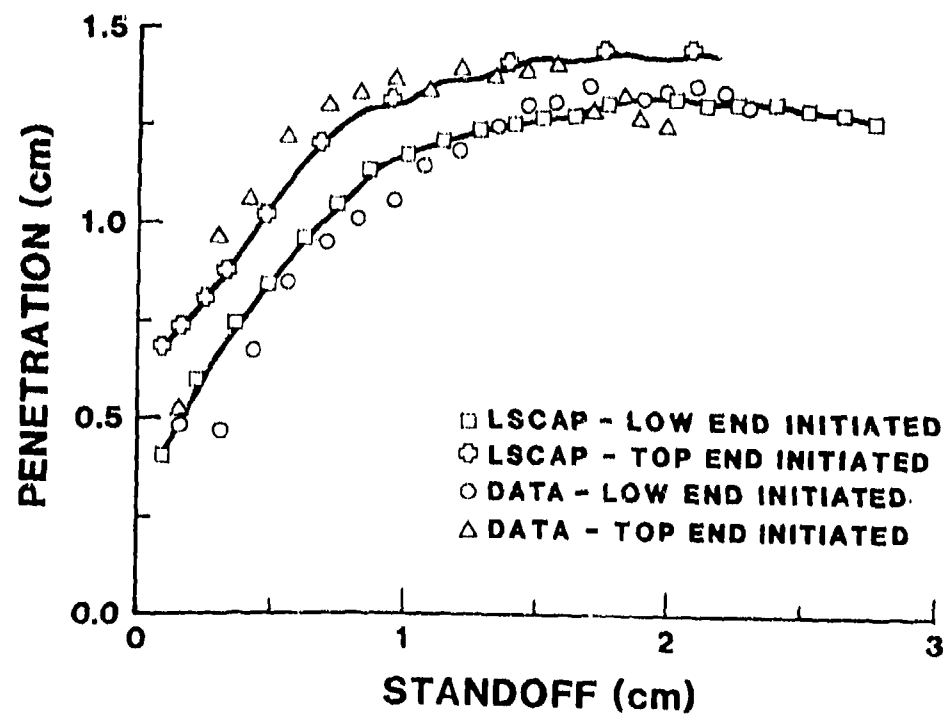
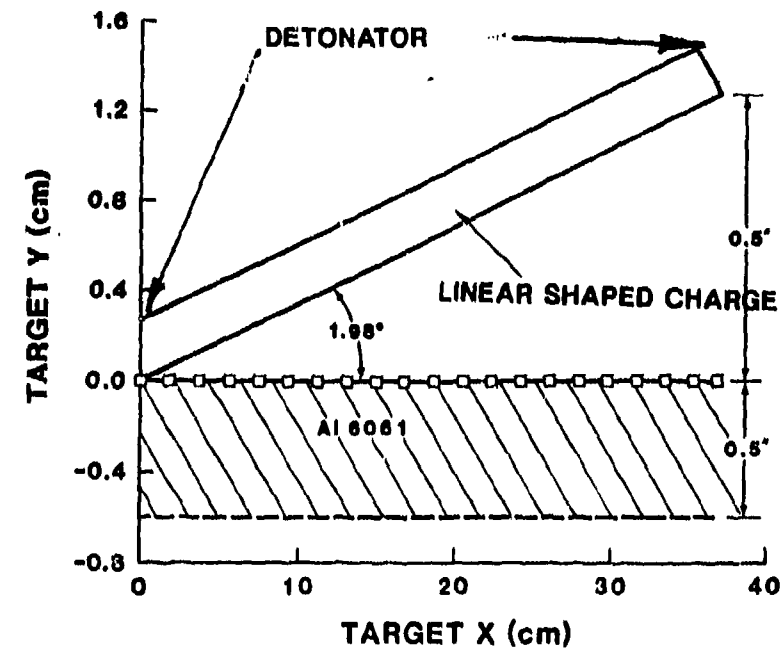


FIGURE 11. LESCA CODE LSC SIMULATION WITH DETONATOR AT MINIMUM VERSUS MAXIMUM STANDOFF



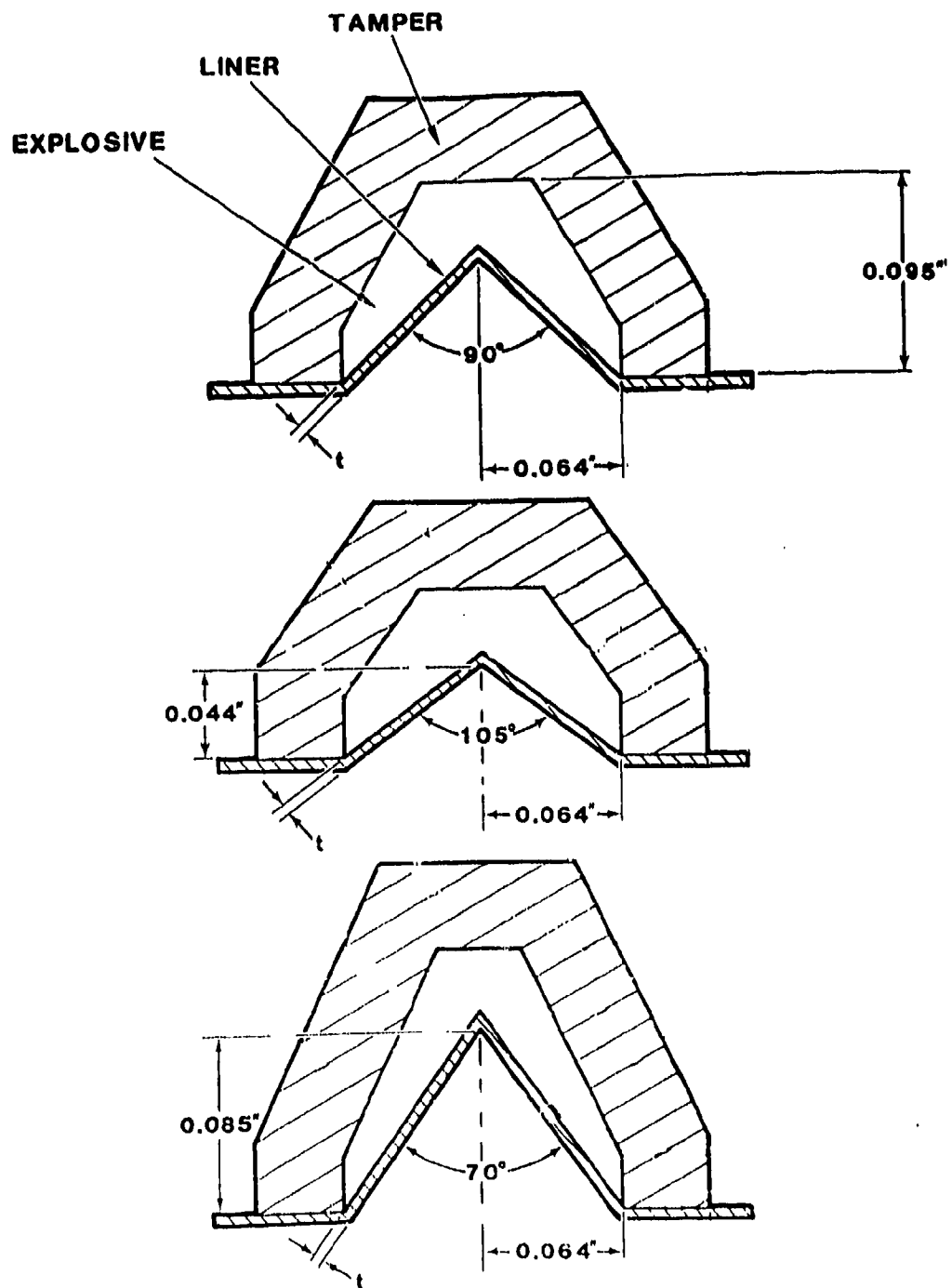
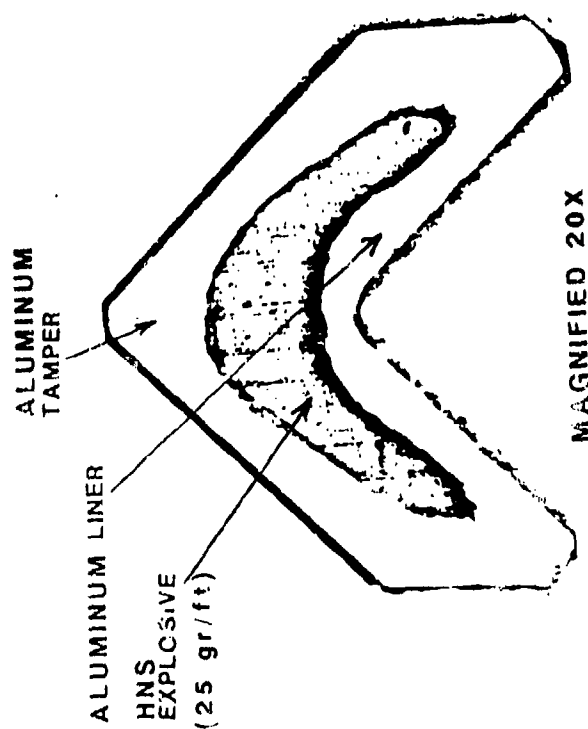
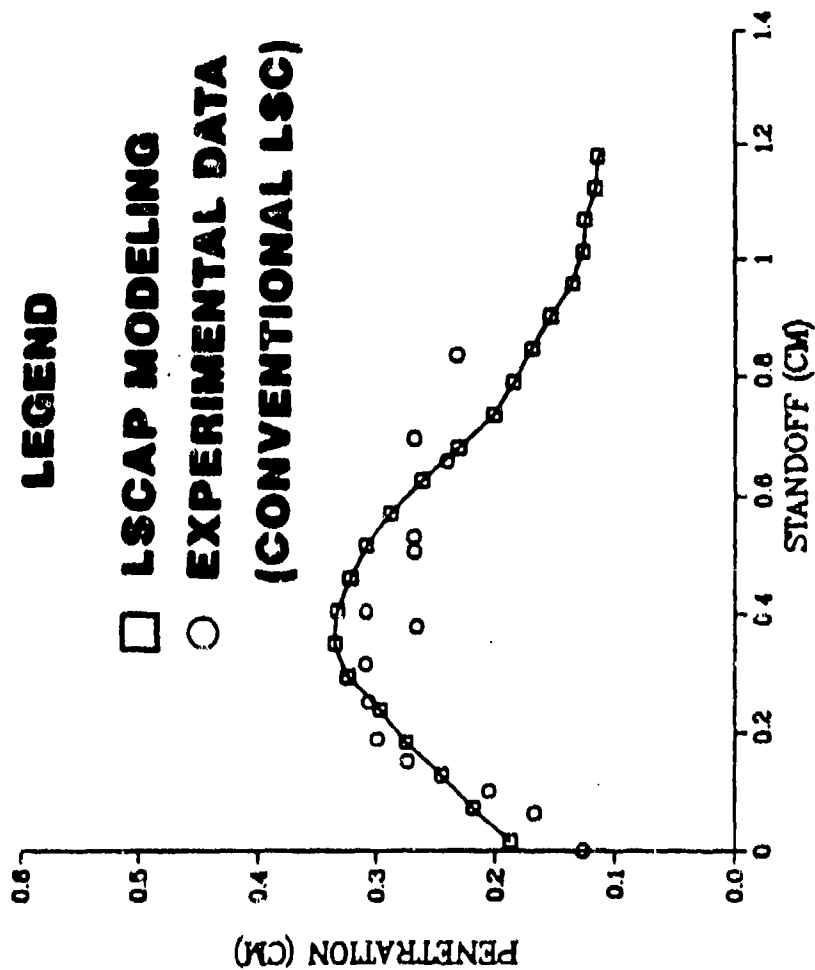


FIGURE 12. "FLANGE" TYPE 25 gr/ft PLSC



**FIGURE 13. CONVENTIONAL LSC PREDICTED JET PENETRATION  
VERSUS STANDOFF COMPARED TO EXPERIMENTAL DATA**

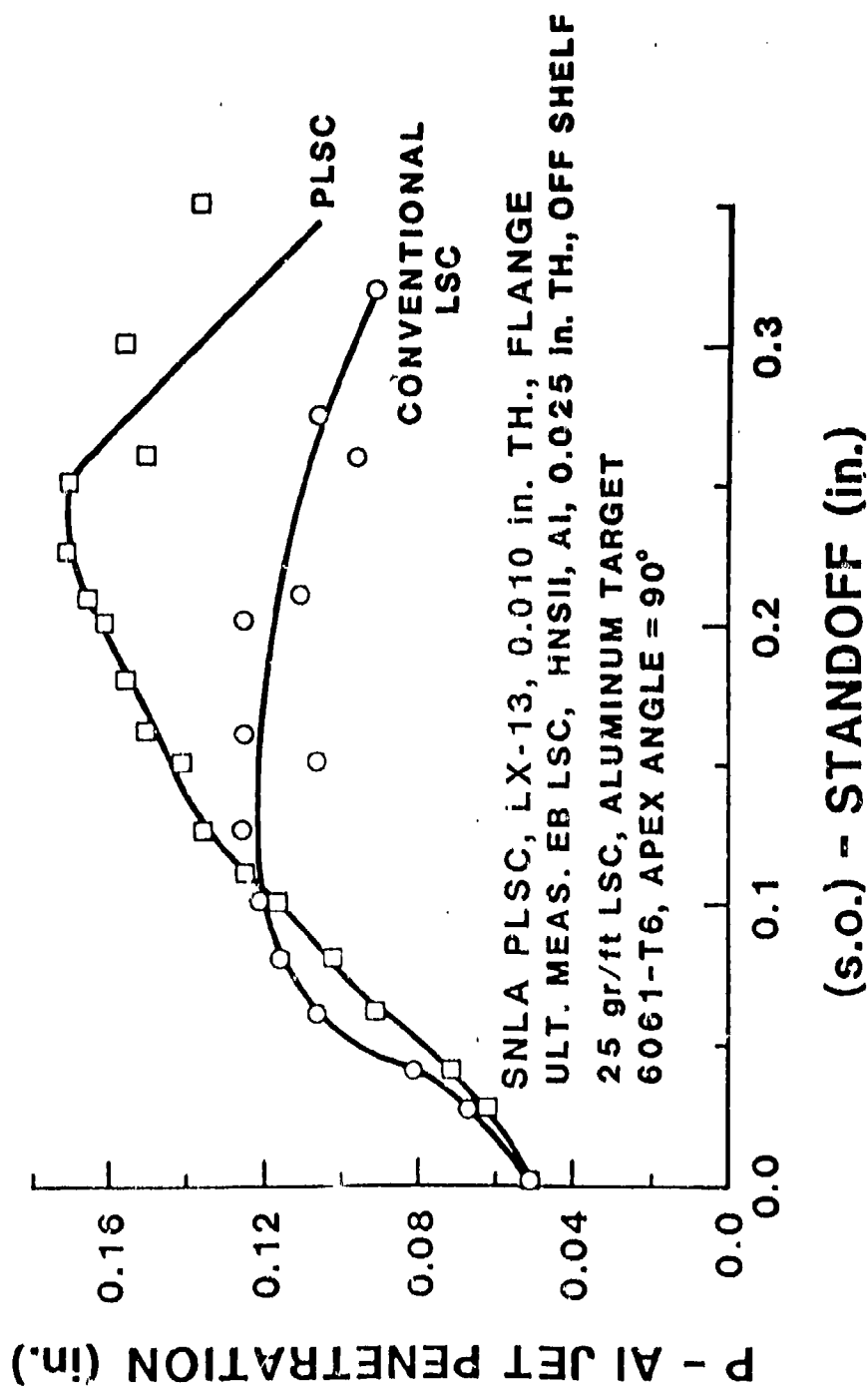
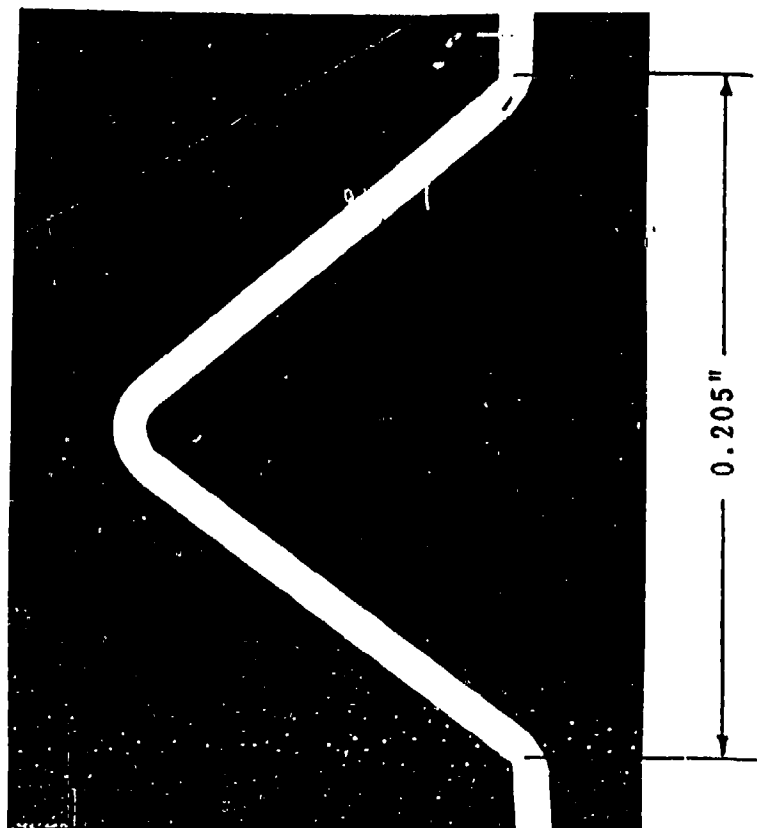
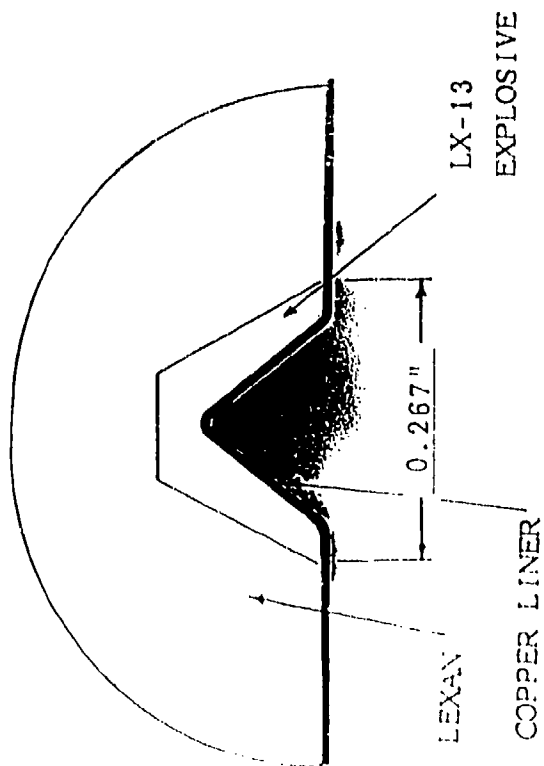
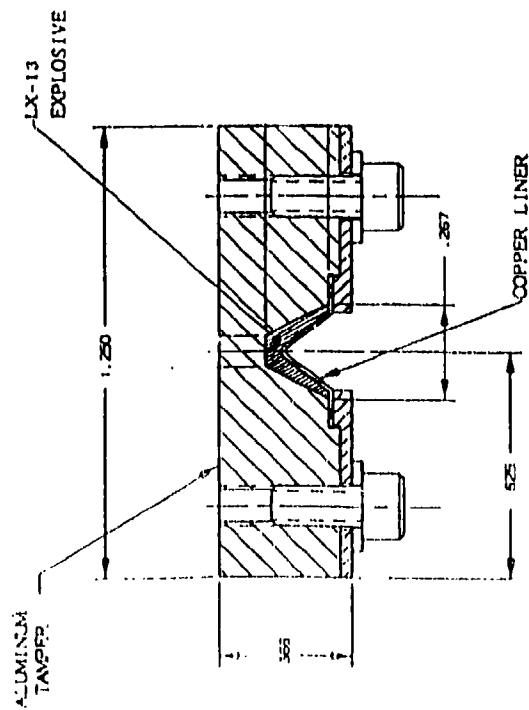
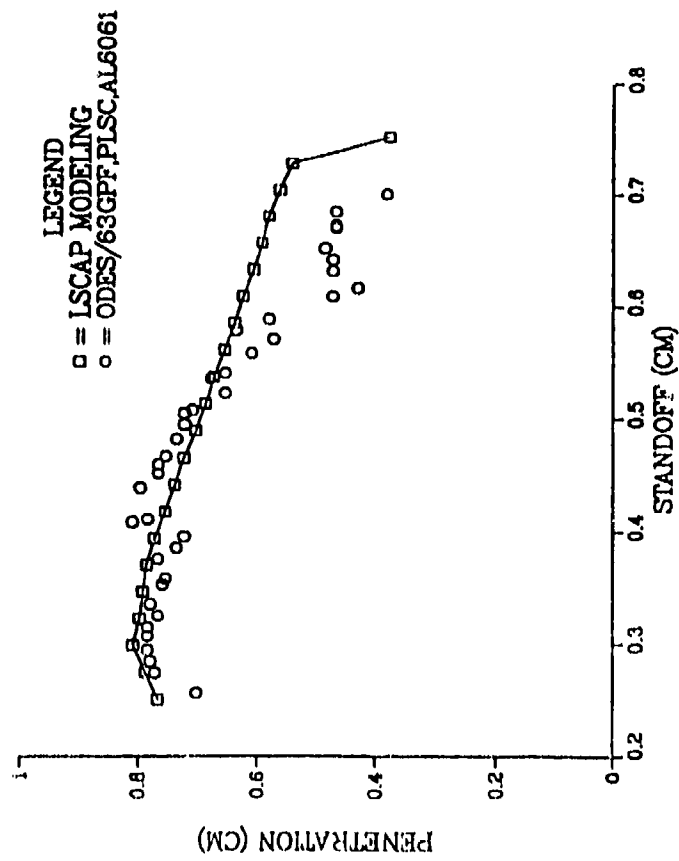


FIGURE 14. JET PENETRATION IN ALUMINUM VERSUS STANDOFF FOR PLSC  
 VERSUS CONVENTIONAL LSC (AI LINER, 90 degree apex, AI TAMPER)



MAGNIFIED: 16 TIMES

FIGURE 15. 65 gr/ft, PLSC7 ACTUAL CROSS-SECTION



**FIGURE 16. 65 gr/ft PLSC 7 CROSS-SECTION AND JET PENETRATION INTO ALUMINUM 6061-T6 VERSUS STANDOFF (LSCA VERSUS MEASURED DATA)**

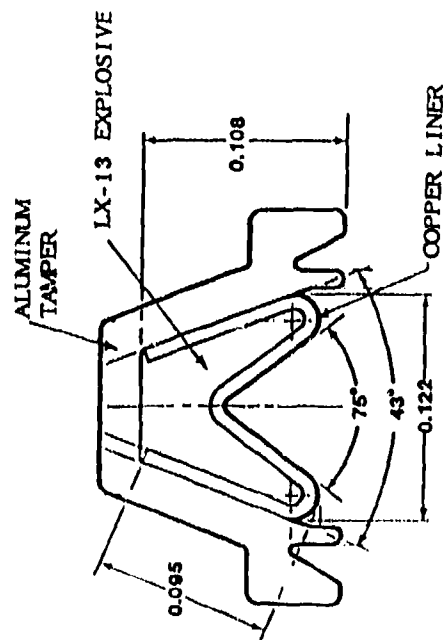
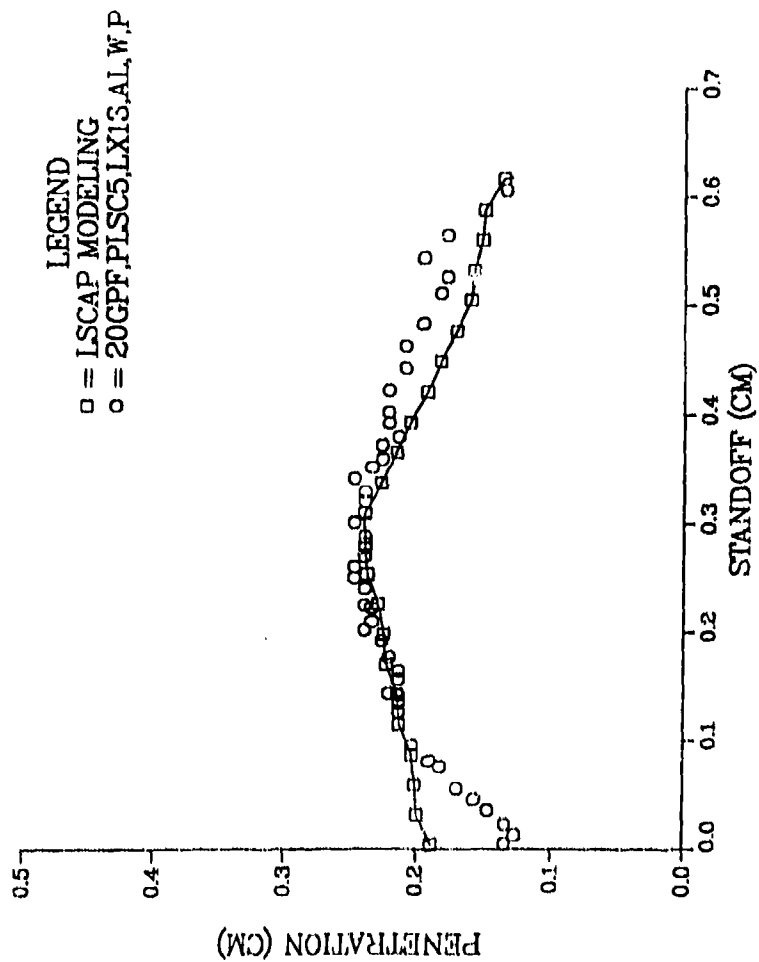
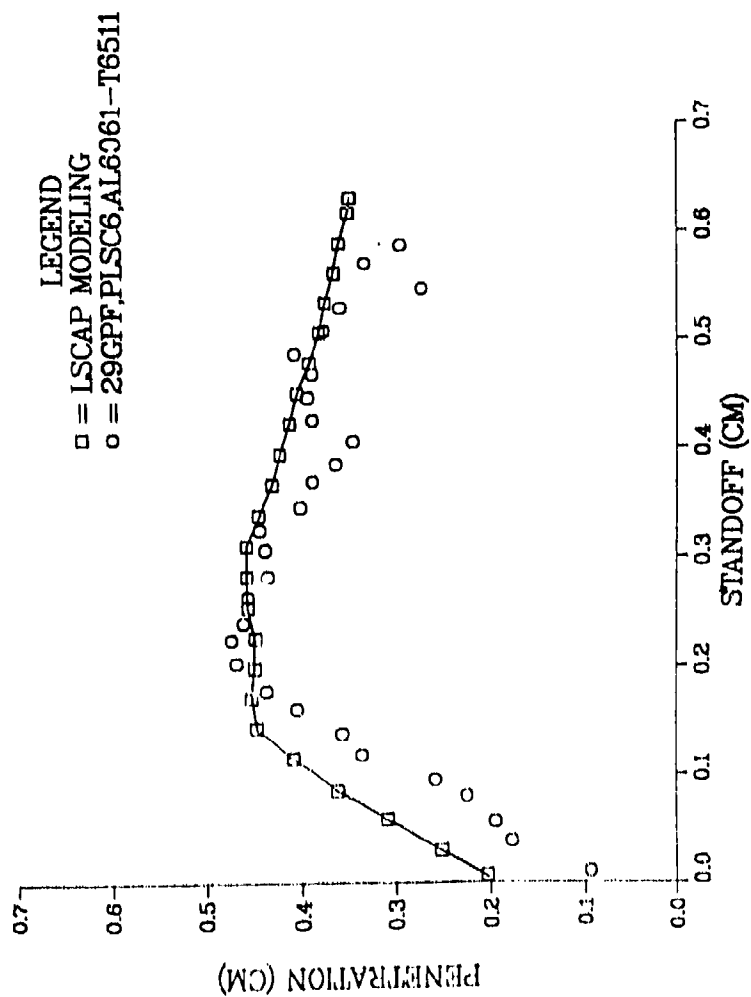
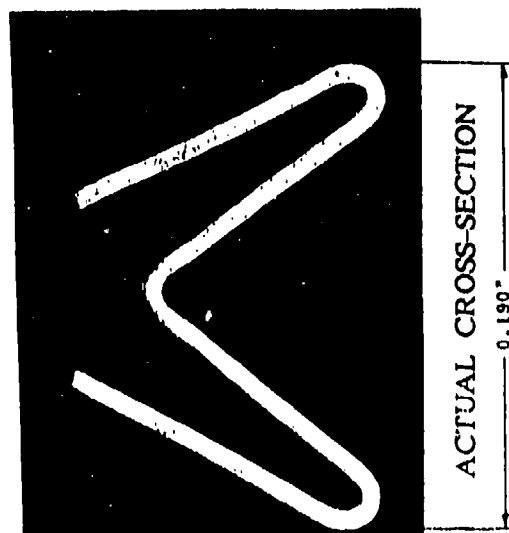
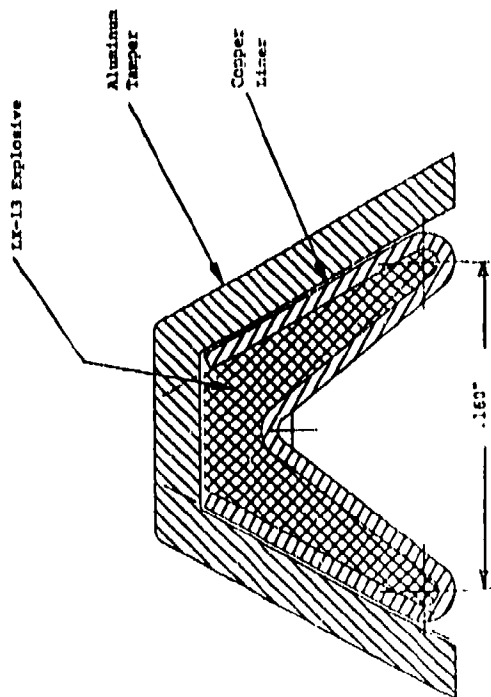


FIGURE 17. 20 gr/ft PLSC JET PENETRATION IN 6061-T6 ALUMINUM  
VERSUS STANDOFF (LESCE VERSUS MEASURED DATA)



**FIGURE 18. 30 gr/ft PLSC6 JET PENETRATION VERSUS STANDOFF  
(LESCA CODE VERSUS MEASURED DATA)**

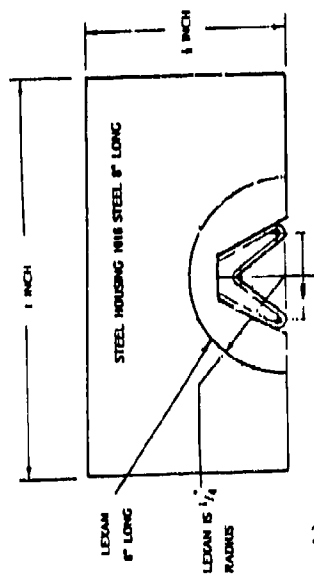
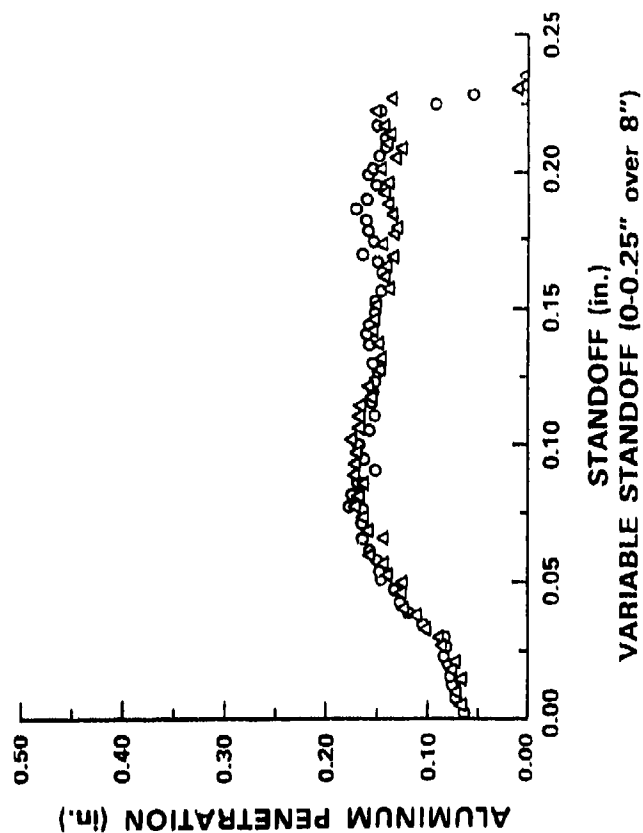


FIGURE 19. REPRODUCIBILITY OF MEASURED 30 gr/ft PLSC6 JET PENETRATION  
VERSUS STANDOFF DATA(TWO TESTS)



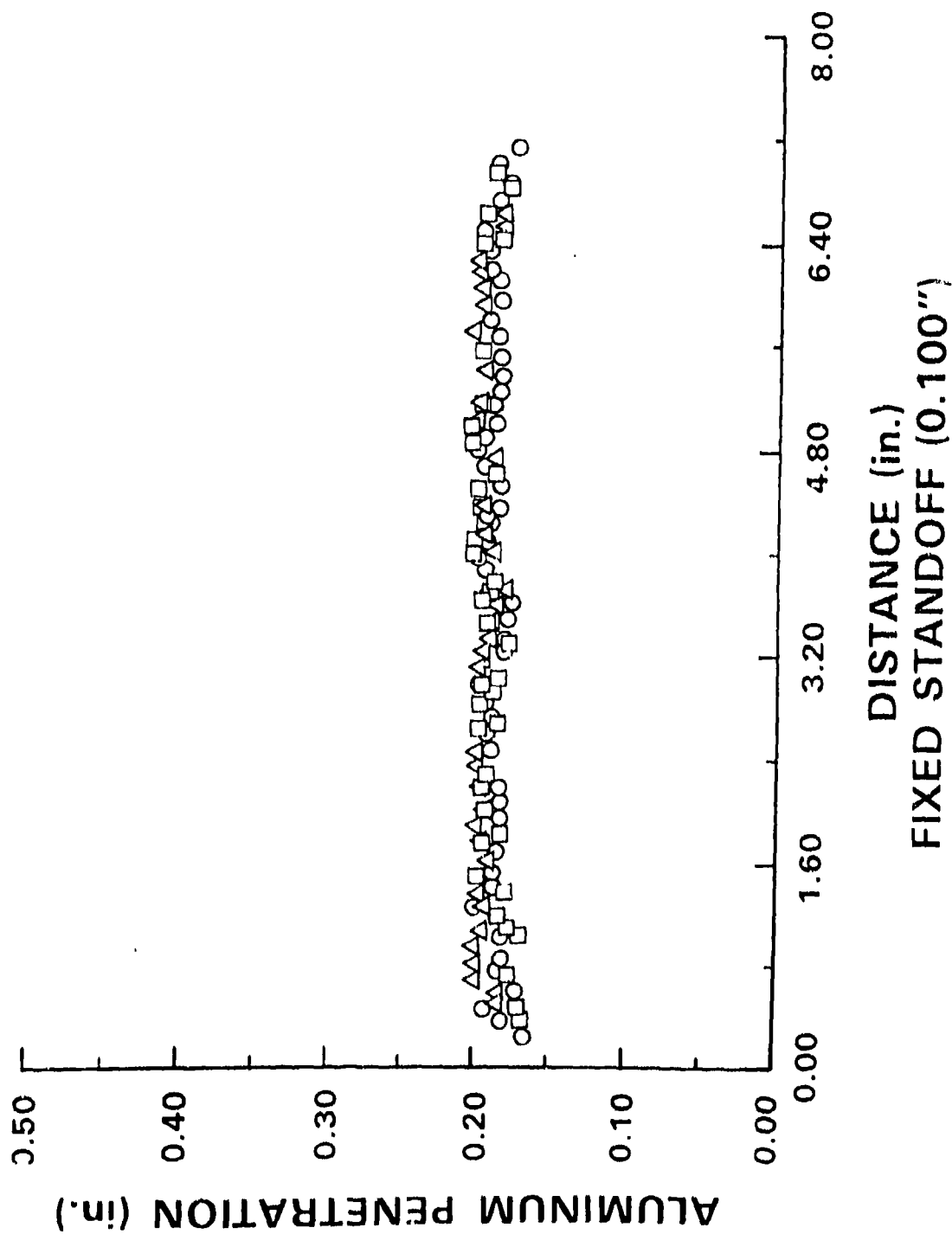


FIGURE 20. REPRODUCIBILITY OF 30 gr/ft PLSC6 JET PENETRATION VERSUS  
DISTANCE ALONG TARGET (CONSTANT STANDOFF, FOAM TAMPER)

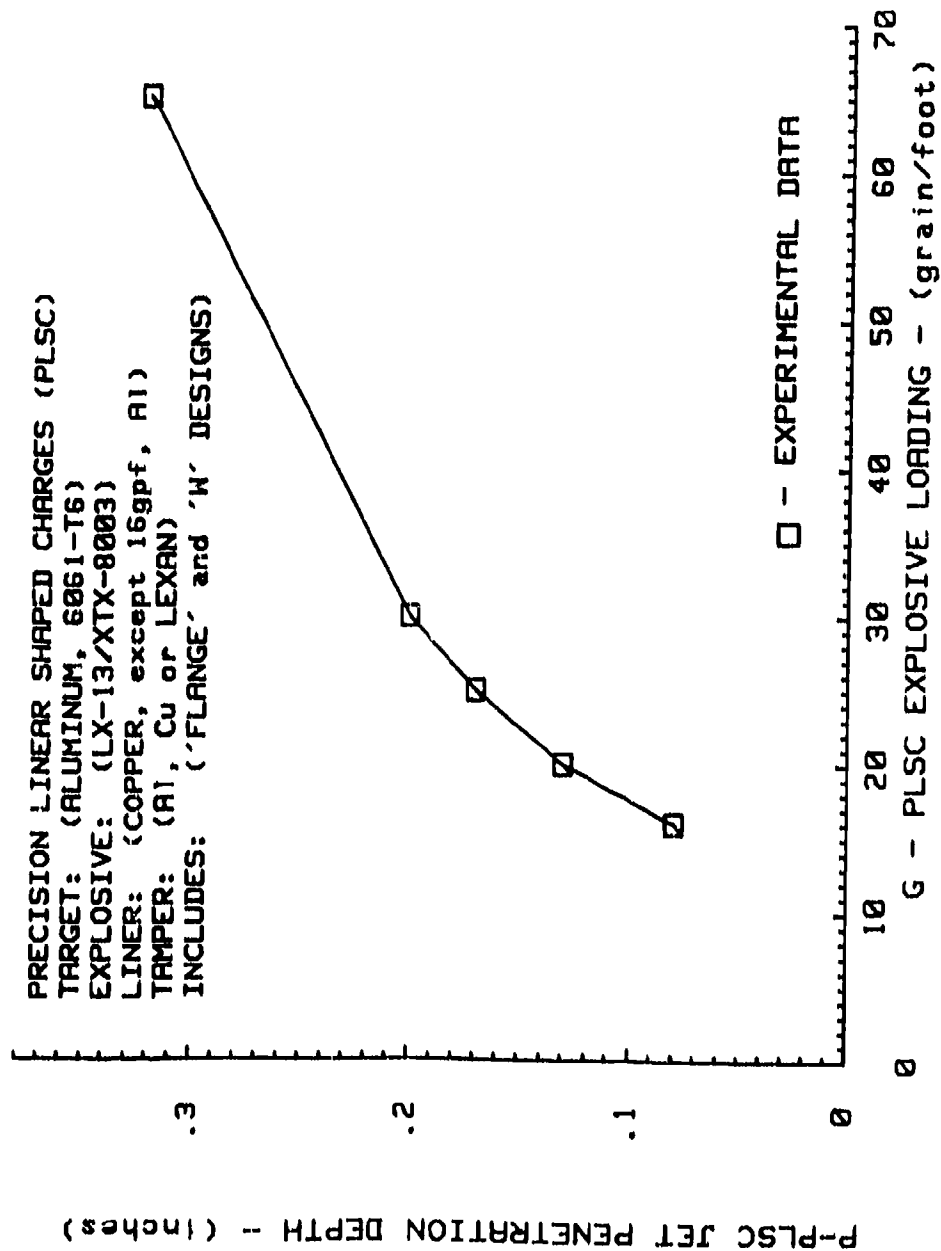


FIGURE 21. PLSC JET PENETRATION DEPTH (P) VERSUS PLSC EXPLOSIVE LOADING (G) FOR ALUMINUM TARGETS

**Distribution:**

8	Mason & Hanger Silas Mason Co., Inc. Pantex Plant Attn: R. Ashcraft D. Garrett S. Hallett P. Kramer T. Meyer R. Slape P. O. Box 30020 Amarillo, TX 79177	1 8523-2 Central Technical Files 5 7141 Technical Library 1 7151 Technical Publications 10 7613-2 Document Processing for DOE/OSTI
	2500 G. N. Beeler 2512 W. J. Andrzejewski 2512 D. R. Begeal 2512 T. S. Casaus 2512 J. G. Harlan 2512 J. A. Merson 2512 F. J. Salas 2512 R. R. Weinmaster 2513 R. A. Benham 2513 F. H. Braaten 2513 J. E. Curzi 2513 S. H. Fischer 2513 T. L. Garcia 2513 M. C. Grubelich 2513 S. M. Harris 2513 D. L. Marchi 2513 D. E. Mitchell 15 2513 M. G. Vigil 2514 R. B. Berry 2514 L. L. Bonzon 2514 W. W. Tarbell 2514 L. J. Weirick 9700 M. M. Newsom 9722 E. G. Kadlec 9723 J. T. Hitchcock 9723 J. M. Holovka 9723 M. L. Lieberman	